# LOCALIZATION OF THE CRYSTALLOGRAPHIC DIRECTIONS OF COMPOSITE MATERIALS FROM WAVESPEED MEASUREMENTS

Christophe Aristégui and Stéphane Baste
Université Bordeaux I
Laboratoire de Mécanique Physique, URA C.N.R.S. 867
351 Cours de la Libération 33405 Talence cedex, France

## INTRODUCTION

The orthorhombic symmetry is considered as general enough to describe the anisotropy of most of the composite materials. The measurement of the anisotropic elasticity constants by ultrasonic techniques usually begins with an assumption that the axes of symmetry are known [1-2]: coincidence of the symmetry axes with the observation axes associated with the thin plate sample is assumed.

We have checked, for a hexagonal medium, that a weak deviation between the observation coordinate system and the principal material coordinate system has notable repercussions on the identification of the elasticity tensor. To avoid this problem, it is necessary to do no assumption on the superposition between the observation axes and the crystallographic directions.

Consequently, the model chosen for the apparent symmetry is triclinic: twenty-one stiffnesses (theoretically non-independent) are determined, and then the crystallographic directions are identified from the wavespeed measurements only. These directions are reconstructed separately. If three directions exist and are mutually nearly orthogonal, then they must coincide with the principal coordinate system. This frame is then searched from only the experimental wavespeed measurements. The nine moduli of an orthorhombic material can therefore be accurately identified. This method is tested on experimental phase velocities in a Carbon Epoxy composite.

## IDENTIFICATION OF THE ELASTICITY CONSTANTS

The phase velocities of an elastic plane wave are the solution of the well-known Christoffel equation [3]:

$$\det\left|\Gamma_{ik} - \rho V^2 \partial_{ik}\right| = 0 \ , \qquad (1)$$

*Review of Progress in Quantitative Nondestructive Evaluation, Vol. 16*
Edited by D.O. Thompson and D.E. Chimenti, Plenum Press, New York, 1997

with $\Gamma_{ij}=C_{ijkl}\, n_k\, n_l$ (i, j, k, l=1, 2, 3) and where $\rho$ is the density, **n** is the unit vector in the wave propagation direction, V is the phase velocity of ultrasonic waves in the medium, $C_{ijkl}$ is the elasticity constants of an anisotropic medium and $\delta_{ij}$ is the Kronecker symbol. By inverting Equation (1), the material properties ($C_{ijkl}$) can be determined from phase velocity measurements in a suitable set of propagation directions [2, 4-5]. Wavespeed measurements are performed by using ultrasonic pulses which are transmitted through a plate immersed in water, Figure 1.

## WRONG RECOGNITION OF THE MATERIAL SYMMETRY

To emphasize the effect of a wrong control of the sample positioning, a unidirectional composite is characterized in an observation frame $R'=(\mathbf{x}_1', \mathbf{x}_2', \mathbf{x}_3')$ different from an elasticity principal coordinate system $R^P=(\mathbf{x}_1^P, \mathbf{x}_2^P, \mathbf{x}_3^P)$, which coincides *a priori* with the geometric frame R, Figures 1 and 2. The deviation between R' and $R^P$ has been chosen slight to reproduce the possible experimental error. The density of the studied sample of Carbon Epoxy composite immersed in water is 1.56 g/cm$^3$ and the thickness is 3.45 mm. The stiffness tensor ($C_{IJ}^P$) relative to $R^P$:

$$\left(C_{IJ}^P\right)=\begin{pmatrix} 12.15\pm0.03 & 5.4\pm0.1 & 5.5\pm0.2 & & & \\ & 12.3\pm0.2 & 5.7\pm0.8 & & 0 & \\ & & 130\pm3 & & & \\ & & & 6.8\pm0.1 & & \\ & \text{Sym.} & & & 6.00\pm0.04 & \\ & & & & & 3.48\pm0.04 \end{pmatrix} \text{(GPa)} \quad (2)$$

are determined [5] from the velocity measurements in the data planes $(\mathbf{x}_1, \mathbf{x}_2)$, $(\mathbf{x}_1, \mathbf{x}_3)$ and $(\mathbf{x}_1, \mathbf{45°})$, Figure 1.

R' is obtained from a $\phi^*$-degree rotation of R about $\mathbf{x}_1$ axis, Figure 2. Using the stiffness tensor transformation, the thirteen elasticity constants relative to R' are determined from ($C_{IJ}^P$), Equation (2). From these thirteen "original data", a set of phase velocities was calculated for selected propagation directions. Since R and R' are very close, the angular ranges experimentally accessible in each plane $(\mathbf{x}_1', \mathbf{x}_2')$, $(\mathbf{x}_1', \mathbf{x}_3')$ and $(\mathbf{x}_1', \mathbf{(45°)}')$ are respectively similar to the ones of the planes $(\mathbf{x}_1, \mathbf{x}_2)$, $(\mathbf{x}_1, \mathbf{x}_3)$ and $(\mathbf{x}_1, \mathbf{45°})$. The range of refraction angles for each of these data planes is determined from the experimental velocities [2] measured in this Carbon Epoxy sample. The moduli identification is then performed in R' from this synthetic velocity set.

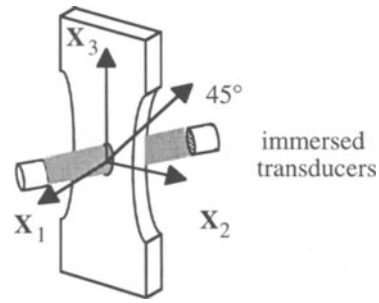


Figure 1. The geometric coordinate system R=($\mathbf{x}_1$, $\mathbf{x}_2$, $\mathbf{x}_3$): $\mathbf{x}_1$ is the normal to the sample.

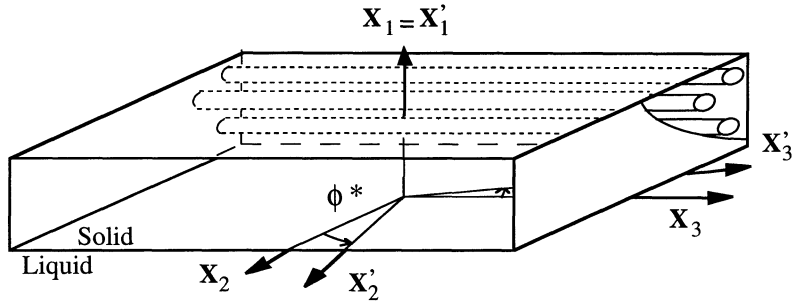


Figure 2. Choice of a non-principal observation coordinate system $R'$ that does not coincide with the geometric coordinate system R of a unidirectional composite.

For any value $\phi^*$ ($\phi^*$=0°, 1°, 2°, 3°, 4° or 5°), we assume that the observation coordinate system $R'$ coincides with $R^p$. The nine moduli $(C'_{IJ})$ are identified from the simulated data in the planes $(\mathbf{x}'_1, \mathbf{x}'_2)$, $(\mathbf{x}'_1, \mathbf{x}'_3)$ and $(\mathbf{x}'_1, \mathbf{(45°)})$. The wrong choice of the stiffness tensor form has principally repercussions on the identification of the moduli $C'_{23}$, $C'_{33}$ and $C'_{44}$, Figure 3 (solid squares). The insensitivity of the confidence intervals to the systematic errors explains that the identified elasticity constants, with their respective confidence interval, do not coincide with the original data. By calculating the engineering constant set from the identified stiffnesses $(C'_{IJ})$, it can be seen that the identification of the Poisson ratios $\nu_{13}$ and $\nu_{23}$ and of the shear modulus $G_{23}$ is very defective when $\phi^*$ increases.

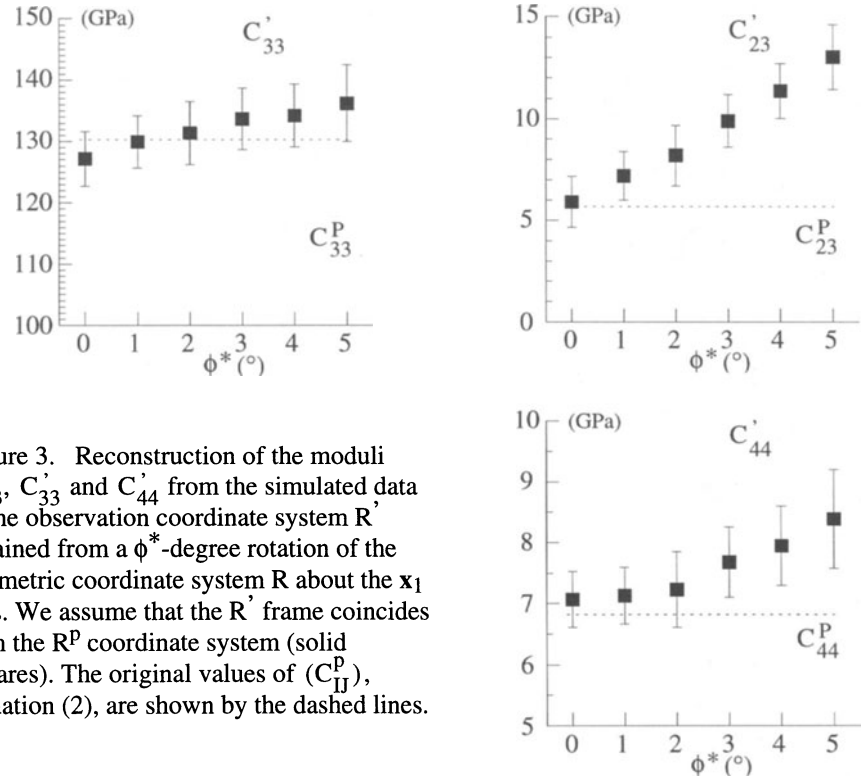


Figure 3. Reconstruction of the moduli $C'_{23}$, $C'_{33}$ and $C'_{44}$ from the simulated data in the observation coordinate system $R'$ obtained from a $\phi^*$-degree rotation of the geometric coordinate system R about the $\mathbf{x}_1$ axis. We assume that the $R'$ frame coincides with the $R^p$ coordinate system (solid squares). The original values of $(C^p_{IJ})$, Equation (2), are shown by the dashed lines.

## RESEARCH OF THE CRYSTALLOGRAPHIC DIRECTIONS

To avoid the problem emphasized previously, we consider that the observation coordinate system R, Figure 1, exhibits the most general anisotropy. The twenty-one equivalent stiffnesses ($C_{IJ}$), Figure 4, are then identified from the wavespeed measurements in the planes ($\mathbf{x}_1$, $\mathbf{x}_2$), ($\mathbf{x}_1$, $\mathbf{x}_3$), ($\mathbf{x}_1$, **45°**) and ($\mathbf{x}_1$, **135°**)[5-6]. Since the ten distinct material symmetries of linear elasticity could be classified [7] by the number and orientation of their planes of symmetry, the location of the crystallographic directions with respect to the observation frame is equivalent to the search for the normals $\mathbf{n}_\pi$ to the planes of symmetry ($\pi$). Identification of the normals $\mathbf{n}_\pi$ is carried out by searching for a monoclinic coordinate system $R^m=(\mathbf{x}_1^m, \mathbf{x}_2^m, \mathbf{x}_3^m)$ in which the form of the stiffness tensor ($C_{IJ}^m$) satisfies the form reported in Figure 5. The normal to the plane of symmetry is then parallel to $\mathbf{x}_1^m$. The $R^m$ identification is therefore equivalent to the reconstruction of this base vector. The two other base vectors $\mathbf{x}_2^m$ and $\mathbf{x}_3^m$ are chosen arbitrarily to form an orthonormal frame. The two Euler angles $\phi$ and $\theta$ are sufficient to locate $R^m$ with respect to the frame R, Figure 6. The periodicity of the angles $\phi$ and $\theta$ is ($\pi/2$). Note that this problem could be resolved using the three Euler angles ($\psi$, $\phi$, $\theta$) [8]. However the sensitivity of this approach for identifying ($\psi$, $\phi$, $\theta$) from wavespeed data is unsatisfactory.

From the conditions [7] on the existence of a symmetry plane, it was proposed [9] to use one particular result deduced from the two symmetric tensors of rank 2, namely the dilatational modulus ($d_{IJ}$) and the Voigt tensor ($V_{IJ}$):

$$V_{IJ} = C_{ikkj}, \qquad d_{IJ} = C_{ijkk}. \tag{3}$$

For monoclinic media these two tensors have a single eigenvector in common (normal to the plane of symmetry). However this approach is independent of the uncertainties of the stiffnesses ($C_{IJ}$). The wavespeed measurements in the planes ($\mathbf{x}_1$, $\mathbf{x}_2$), ($\mathbf{x}_1$, $\mathbf{x}_3$), ($\mathbf{x}_1$, **45°**) and ($\mathbf{x}_1$, **135°**) are therefore introduced in the proposed method. A functional $\pounds(\phi, \theta)$ is built that is minimal for a value of the angular couple ($\phi$, $\theta$) localizing $R^m$ in the observation coordinate system R. To build $\pounds(\phi, \theta)$, the Christoffel equation is rewritten in a current frame $R_{(\phi, \theta)}$ assuming that this frame coincides with a monoclinic coordinate system. However the coefficients ($C_{IJ}$) appear implicitly in $\pounds(\phi, \theta)$ and the uncertainties $I(C_{IJ})$ are not taken into account. The optimal determination of the stiffness tensor ($C_{IJ}^m$) and of the angles ($\phi^m$, $\theta^m$) locating the monoclinic coordinate system with respect to the observation frame R is then carried out from the wavespeed measurements in R. These fifteen unknowns are identified by minimizing the functional $\Im((C_{IJ}^m), (\phi, \theta))$ (built from the Christoffel equation) that only depends on the experimental data. The accuracy of optimization results is estimated calculating the 99% confidence interval [10] associated with all the fifteen unknowns. The functionals $\pounds(\phi, \theta)$ and $\Im((C_{IJ}^m), (\phi, \theta))$ are similar to the ones presented in reference [6] for the location of a principal (or orthorhombic) coordinate system $R^p$.

$$(C_{IJ}) = \begin{bmatrix} C_{11} & C_{12} & C_{13} & C_{14} & C_{15} & C_{16} \\ & C_{22} & C_{23} & C_{24} & C_{25} & C_{26} \\ & & C_{33} & C_{34} & C_{35} & C_{36} \\ & & & C_{44} & C_{45} & C_{46} \\ & \text{Sym.} & & & C_{55} & C_{56} \\ & & & & & C_{66} \end{bmatrix}$$

Figure 4. The triclinic stiffness tensor.

$$(C_{IJ}) = \begin{bmatrix} C_{11} & C_{12} & C_{13} & C_{14} & & \\ & C_{22} & C_{23} & C_{24} & & 0 \\ & & C_{33} & C_{34} & & \\ & & & C_{44} & & \\ & \text{Sym.} & & & C_{55} & C_{56} \\ & & & & & C_{66} \end{bmatrix}$$

Figure 5. The monoclinic stiffness tensor.

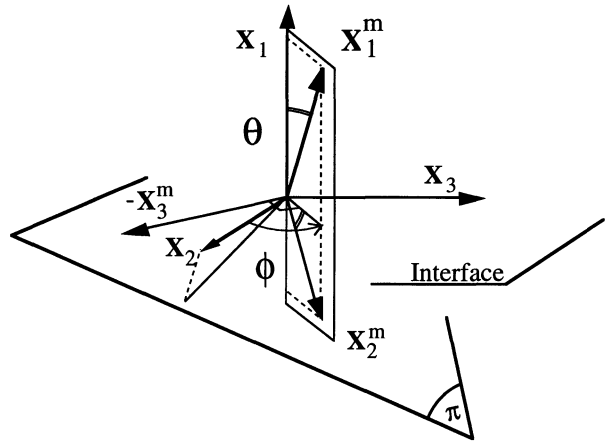


Figure 6. Location of the normal $\mathbf{n}_\pi$ to the plane ($\pi$) of symmetry with respect to the geometric frame R by the two Euler angles $\phi$ and $\theta$ relative to the rotations about the $\mathbf{x}_1$ axis and the transformed $\mathbf{x}_3$ axis respectively. $\mathbf{n}_\pi$ is along the first base vector $\mathbf{x}_1^m$.

The search for a crystallographic direction has been carried assuming the existence of $R^m$. Using the stiffness transformation laws, the moduli $(C_{IJ})^{computed}$ relative to the observation frame R can be calculated from the optimal couple $((C_{IJ}^m), (\phi^m, \theta^m))$. The good agreement between $(C_{IJ})^{computed}$ and the stiffness tensor $(C_{IJ})$ identified from the experimental data allows one to discuss the $R^m$ existence. The comparison between $(C_{IJ})^{computed}$ and the stiffness tensor $(C_{IJ})$ can also be performed by calculating the deviation $\Delta$ [9]:

$$\Delta = \sqrt{\left(C_{ijkl} - C_{ijkl}^{computed}\right)^2 \Big/ \left(C_{ijkl}\right)^2}. \qquad (4)$$

## APPLICATION TO A UNIDIRECTIONAL CARBON EPOXY SAMPLE

To validate the experimental reconstruction of material symmetry, the experiment is done on the Carbon Epoxy sample whose fibrous reinforcement direction is known (along the direction $\mathbf{x}_3$). The chosen observation coordinate system $R''=(\mathbf{x}_1'', \mathbf{x}_2'', \mathbf{x}_3'')$ is obtained from a 30-degree rotation of R about $\mathbf{x}_1$ axis followed by a 10-degree rotation about the transformed $\mathbf{x}_3''$ axis ($\mathbf{x}_3'$), Figure 7.

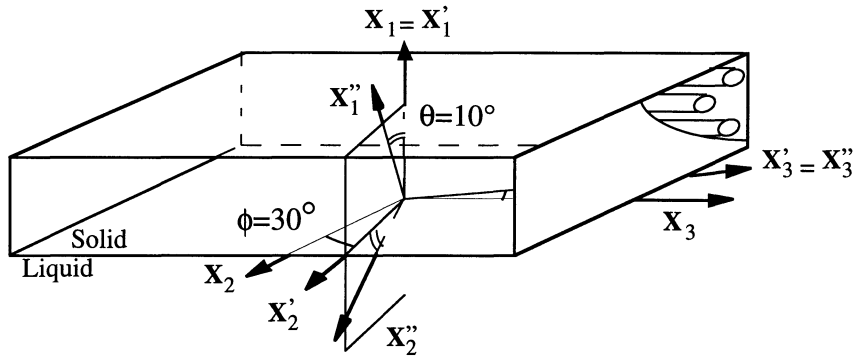


Figure 7. Choice of a non-principal observation coordinate system R" that does not coincide with the geometric coordinate system R of a unidirectional composite.

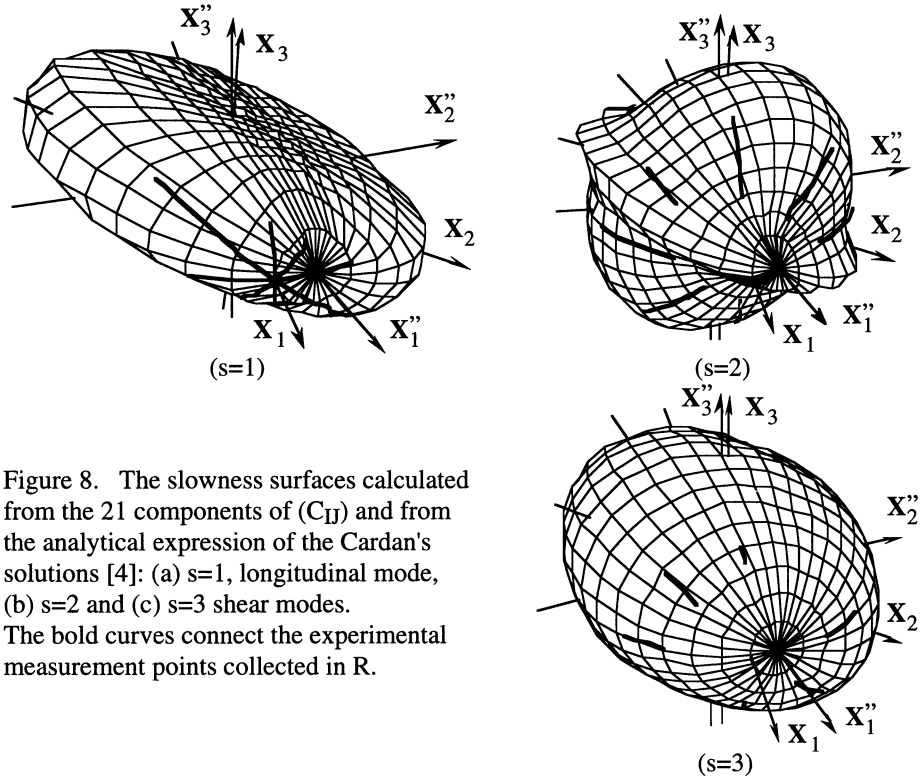


Figure 8. The slowness surfaces calculated from the 21 components of ($C_{IJ}$) and from the analytical expression of the Cardan's solutions [4]: (a) s=1, longitudinal mode, (b) s=2 and (c) s=3 shear modes. The bold curves connect the experimental measurement points collected in R.

However, it is difficult to simulate such a frame R" of propagation in the material from a rotation that is predetermined and applied to the apparatus emitting the ultrasonic waves. The base vector $\mathbf{x}_1^{"}$ is indeed different from the normal to the sample $\mathbf{x}_1$ and according to Snell-Descartes' laws [3] corresponds to several incident waves. These difficulties disappear as soon as the normal to a sample with triclinic symmetry, coincides with a base vector of the observation coordinate system R".

The study is carried out from the experimental velocities measured for positive and negative incident angles in the data planes ($\mathbf{x}_1$, **30°**), ($\mathbf{x}_1$, **120°**), ($\mathbf{x}_1$, **75°**) and ($\mathbf{x}_1$, **165°**). The twenty-one components of the equivalent stiffness tensor in R":

$$\left(C_{IJ}^{"}\right)=\begin{pmatrix} 12.24\pm0.02 & 5.4\pm0.2 & 6.2\pm0.2 & 0.27\pm0.07 & 0.43\pm0.02 & 0.28\pm0.02 \\ & 20.9\pm0.5 & 23.9\pm0.5 & 13.1\pm0.3 & 1.9\pm0.1 & 1.3\pm0.1 \\ & & 83.4\pm1.0 & 36.4\pm0.5 & 6.4\pm0.2 & 3.2\pm0.2 \\ & & & 25.4\pm0.3 & 3.5\pm0.1 & 2.2\pm0.1 \\ & \text{Sym.} & & & 5.9\pm0.1 & 1.43\pm0.03 \\ & & & & & 4.4\pm0.1 \end{pmatrix} \text{(GPa)} \quad (5)$$

are determined from these data collected in R and then related to R", Figure 8.

The material anisotropy of the Carbon Epoxy sample is identified from the set of experimental data reported in Figure 8. First, the crystallographic directions are located with respect to R" by the two angles ($\phi$, $\theta$). The plot of the functional $\pounds(\phi, \theta)$, Figure 9, emphasizes three minima that can coincide with the normal $\mathbf{n}_\pi$ to be identified. From these three assessments, the three optimal solutions, minimizing the funtional $\Im((C_{IJ}^{m}), (\phi, \theta))$, are summarized in Table 1.

Table 1. Reconstruction of both the angles ($\phi^m$, $\theta^m$) and the stiffness tensor ($C_{IJ}^m$), from the experimental phase velocities for a Carbon Epoxy composite. The numbers in the parentheses indicate the confidence interval associated with each identified amount.

| | $\phi^m$ | $\theta^m$ | $C_{11}^m$ | $C_{12}^m$ | $C_{13}^m$ | $C_{14}^m$ | $C_{22}^m$ | $C_{23}^m$ | $C_{24}^m$ | $C_{33}^m$ | $C_{34}^m$ | $C_{44}^m$ | $C_{55}^m$ | $C_{56}^m$ | $C_{66}^m$ |
|---|---|---|---|---|---|---|---|---|---|---|---|---|---|---|---|
| | (degree) | | (GPa) | | | | | | | | | | | | |
| $(\mathbf{n}_\pi)^1$ | 60.8 | 85.1 | 131 | 5.5 | 5.7 | 0.0 | 12.16 | 5.4 | 0.04 | 12.3 | -0.02 | 3.48 | 6.9 | 0.14 | 5.99 |
| | (0.1) | (0.1) | (2) | (0.1) | (0.5) | (0.2) | (0.02) | (0.1) | (0.02) | (0.2) | (0.02) | (0.02) | (0.1) | (0.02) | (0.03) |
| $(\mathbf{n}_\pi)^2$ | -30.0 | 81.3 | 12.3 | 5.5 | 5.7 | -0.0 | 12.24 | 6.3 | -0.52 | 129 | -9.7 | 6.77 | 6.9 | -0.29 | 3.51 |
| | (0.2) | (0.7) | (0.2) | (0.1) | (0.5) | (0.1) | (0.02) | (0.1) | (0.02) | (2) | (0.2) | (0.03) | (0.1) | (0.01) | (0.03) |
| $(\mathbf{n}_\pi)^3$ | 0.0 | -10.0 | 12.15 | 5.3 | 5.7 | -0.1 | 21.4 | 24.4 | 13.6 | 83 | 36.9 | 26.0 | 5.3 | 1.11 | 4.2 |
| | (1.5) | (0.5) | (0.02) | (0.1) | (0.2) | (0.1) | (1.5) | (1.3) | (1.5) | (4) | (0.5) | (1.3) | (0.1) | (0.04) | (0.1) |

For each of the three solutions, the slight deviation $\Delta$ (=1.1%), Equation (4), between the moduli ($C_{IJ}$) and the stiffness tensor $(C_{IJ}^{"})^{computed}$ equivalent to the optimal solution (($C_{IJ}^m$), ($\phi^m$, $\theta^m$)) in R" validates the existence of the three identified crystallographic directions $(\mathbf{n}_\pi)^k$, k=1, 2, 3. The expression of the unit vectors $\mathbf{x}_1^m$ defined by ($\phi^m$, $\theta^m$) in R:

$$(\mathbf{n}_\pi)^1 = \mathbf{x}_3, \qquad (\mathbf{n}_\pi)^2 = \mathbf{x}_2, \qquad (\mathbf{n}_\pi)^3 = \mathbf{x}_1, \tag{6}$$

shows that the three principal axes $\mathbf{x}_1^p$, $\mathbf{x}_2^p$ and $\mathbf{x}_3^p$, Figure 7, have been independently reconstructed. This is confirmed by the comparison of the elasticity constants $C_{11}^p$(=12.15), $C_{22}^p$(=12.3), $C_{33}^p$(=130 GPa), Equation (2), and the three moduli $C_{11}^m$ associated with the directions $(\mathbf{n}_\pi)^1$, $(\mathbf{n}_\pi)^2$, $(\mathbf{n}_\pi)^3$ respectively, Table 1. The experimental location of a normal to a plane of symmetry can be accurately achieved.

Let us searching for the elasticity principal coordinate system $R^p$ located with respect to the observation frame R" by the three Euler angles ($\psi$, $\phi$, $\theta$) [11]. $\psi$ is relative to the rotation about the $\mathbf{x}_3$ axis. The process of $R^p$ reconstruction is similar to that described previously for the location of a monoclinic frame. The number of optimal unknowns is equal to twelve (3 angles and 9 $C_{IJ}$). The optimal results of the $R^p$ reconstruction are summarized in Table 2. The slight deviation ($\Delta$ =1.1%) between the moduli ($C_{IJ}^{"}$) and the stiffness tensor $(C_{IJ}^{"})^{computed}$ equivalent to the optimal solution (($C_{IJ}^p$), ($\psi^p$, $\phi^p$, $\theta^p$)) in R" allows one to verify the $R^p$ existence. The expression of the base vectors of the identified frame $R^p$ in R:

$$\mathbf{x}_1^p = \mathbf{x}_1, \qquad \mathbf{x}_2^p = \mathbf{x}_2, \qquad \mathbf{x}_3^p = \mathbf{x}_3. \tag{7}$$

and the coincidence between the tensor ($C_{IJ}^p$), Equation (2), and the optimal tensor ($C_{IJ}^p$) (determined simultaneously with $\delta^p$, Table 2) confirms the applicability of the reconstruction method.

Table 2. Reconstruction of both the angles ($\psi^p$, $\phi^p$, $\theta^p$) and the stiffness tensor ($C_{IJ}^m$), from the experimental phase velocities for a Carbon Epoxy composite.

| $\psi^p$ | $\phi^p$ | $\theta^p$ | $C_{11}^p$ | $C_{12}^p$ | $C_{13}^p$ | $C_{22}^p$ | $C_{23}^p$ | $C_{33}^p$ | $C_{44}^p$ | $C_{55}^p$ | $C_{66}^p$ |
|---|---|---|---|---|---|---|---|---|---|---|---|
| (degree) | | | (GPa) | | | | | | | | |
| -10.0 | -29.6 | 0.0 | 12.15 | 5.5 | 5.5 | 12.3 | 5.7 | 131 | 6.9 | 5.97 | 3.48 |
| (0.1) | (0.1) | (0.6) | (0.02) | (0.1) | (0.1) | (0.2) | (0.5) | (2) | (0.1) | (0.03) | (0.03) |

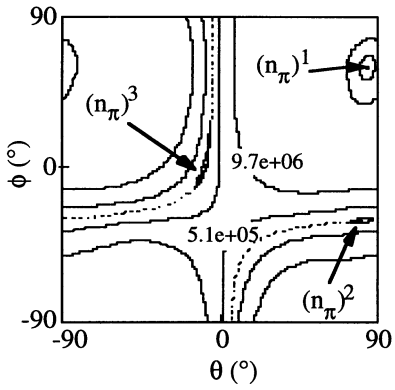


Figure 9. Isovalues of the functional £(ϕ, θ) calculated from ($C''_{IJ}$), Equation (5) and the experimental data, Figure (8). Three minima are clearly visible.

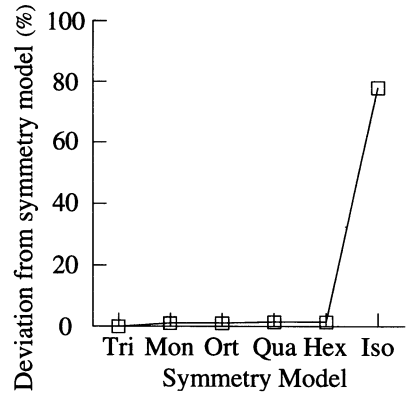


Figure 10. The more probable symmetry for a unidirectional composite whose characterization has been performed in a non-principal coordinate system.

However the material symmetry can be higher than the orthorhombic symmetry. For each classical symmetry, a stiffness tensor ($C_{IJ}^{model}$) whose components satisfy the relation peculiar to these symmetries is built from the moduli ($C_{IJ}^{p}$). For each tensor ($C_{IJ}^{model}$) reconstructed in this way in $R^p$, the equivalent tensor $(C_{IJ})^{computed}$ in R is obtained from ($\psi^p$, $\phi^p$, $\theta^p$). The calculation of the deviation $\Delta_{model}$, Equation (4), between $(C_{IJ})^{computed}$ and the moduli ($C''_{IJ}$), Equation (5), allows one to quantify the deviation from the isotropic (Iso), hexagonal (Hex) and quadratic (Qua) models, Figure 10. The deviations calculated at the time of the search for the frames $R^m$ (Mon) and $R^p$ (Ort) are also reported. Clearly it appears that the more probable material symmetry is the hexagonal symmetry. Every direction lying in the isotropic plane ($\mathbf{x}_1^p$, $\mathbf{x}_2^p$) must correspond to a normal to a plane of symmetry. Each of these directions is expressed in the observation coordinate system R'' with the two angles (ϕ, θ) defined Figure 6. This set of angles couples is shown in Figure 9 by dashed lines. If the material symmetry is exactly hexagonal, these two curves must superimposed on the set of minima of the functional £(ϕ, θ). Although a decrease of £(ϕ, θ) appears around these curves, only two points of these lines minimize the functional £(ϕ, θ). The experimental errors on velocity measurements or the quasi-hexagonal symmetry of the sample can explain this behavior.

## REFERENCES


1. J. Roux, B. Hosten, B. Castagnède and M. Deschamps, Rev. Phys. Appl. 20, 351 (1985).
2. S. Baste and B. Hosten, Rev. Phys. Appl. 25, 161 (1990).
3. B. A. Auld, *Acoustic Fields and Waves in solids* (Wiley-Interscience, New York, 1973).
4. S. I. Rokhlin and W. Wang, J. Acoust. Soc. Am. 91, 3303 (1992).
5. C. Aristégui and S. Baste, submitted to J. Acoust. Soc. Am.
6. C. Aristégui and S. Baste, in *Review of Progress in QNDE*, Vol. 15B, eds D. O. Thompson and D. E. Chimenti (Plenum press, New York, 1995), p. 1677.
7. S. C. Cowin and M. M. Mehrabadi, Q. J. Mech. appl. Math. 40, 451 (1987).
8. C. Aristégui and S. Baste, *Proceedings of the Ultrasonics World Congress 1995*, Vol. 1, p. 463.
9. R. Artz, "A study of general anisotropic elasticity in rocks by wave propagation Theorical and experimental apects", PH.D. Paris VI (1993).
10. A. Gourdin and M. Boumahrat, *Méthodes numériques appliquées* (Lavoisier, Paris, 1983).
11. B. Castagnède, J. T. Jenkins, W. Sachse and S. Baste, J. Appl. Phys. 67, 2753 (1990).